Final Draft

of the original manuscript

Inácio, P.; Camacho, E.; Schell, N.; Braz Fernandes, F.; Oliveira, J.; Santos, T.:

Production and characterization of functionally graded NiTi shape memory alloys by Joule effect.

In: Journal of Materials Processing Technology. Vol. 285 (2020) 116803.

First published online by Elsevier: 17.06.2020

https://dx.doi.org/10.1016/j.jmatprotec.2020.116803

Production and characterization of functionally graded NiTi shape memory alloys by Joule effect

Patrick. L. Inácio [A], Edgar F. Camacho [B], N. Schell [C], F. M. Braz Fernandes [B], J. P. Oliveira [A], Telmo G. Santos [A]

[A] UNIDEMI, Department of Mechanical and Industrial Engineering, NOVA School of Science and Technology, Universidade NOVA de Lisboa, 2829-516 Caparica, Portugal.

[B] CENIMAT/I3N, Department of Materials Science, NOVA School of Science and Technology, Universidade NOVA de Lisboa, 2829-516 Caparica, Portugal.

[C] Helmholtz-Zentrum Geesthacht, Institute of Materials Research, Max-Planck-Str. 1, Geesthacht, 21502, Germany.

Abstract

Localized heat treatments via Joule effect were performed on cold-drawn NiTi strips to produce a functionally graded material (FGM). Three zones where locally heat treated at 300, 350, and 400 °C for 10 min followed by air cooling. Multiscale and multiphenomena characterization of the obtained FGM was performed through infrared temperature testing, four-point probe and eddy current testing, mechanical testing and synchrotron X-Ray diffraction. The effect of these localized heat treatments is clearly observed by different techniques. The use of these short and localized heat treatments avoids the need of highly expensive manufacturing routes typically used to obtain the same effect on NiTi shape memory alloys, thus opening new routes for processing these advanced engineering alloys.

Keywords: Shape Memory Alloys (SMA), Heat Treatment, Joule effect, Functionally Graded Material (FGM), Characterization.

1. Introduction

Shape memory alloys are a class of functional materials characterized by their functional properties: shape memory effect and superelasticity. These occur due to a thermodynamically reversible martensitic transformation. The application of such materials spans over a wide range of applications: from the biomedical and aerospace fields to civil engineering, for example.

Several types of shape memory alloys exist, being NiTi- and Cu-based ones the most used nowadays. In terms of industrial applications, NiTi is the predominant alloy system owing to its stable and well understood microstructure and mechanical properties. In order to further expand the current applications of these advanced functional materials there is a need to create functionally graded properties to provide engineers and designers with more freedom when developing complex shaped structures. One way to control the transformation characteristics of NiTi-based alloys, and therefore, their mechanical properties, is through the use of heat treatments. In Ni-rich NiTi alloys, low temperature heat treatments, i.e. typically below 450 °C, are used for precipitation of Ni_4Ti_3 which can promote the formation of R-phase and at the same time modify the transformation temperatures of the alloy. The creation of functionally graded parts using conventional furnace heat treatments is difficult owing to the need to impose different heat treatment conditions, i.e. time and/or temperature, so that precipitation of desired phases or other microstructural changes (recrystallization and/or grain grow) can occur in a discrete, localized and controlled way.

Microstructural control by thermal heat treatments without the use of conventional furnaces can be performed using Joule heating. This approach was demonstrated in the work of Wang *et al.* (2009) in NiTi shape memory alloys. Subsequently, Yang *et al.* (2010) and Kang *et al.* (2010), further expanded the concept to Ni-Ti-Cu alloys.

Meng *et al.* (2013), Meng *et al.* (2016) and Sun *et al.* (2018) also used electrical current to perform localized heat treatments in NiTi and correlated the process parameters (current and time) with the obtained microstructure and mechanical properties of the processed wires. This approach was effective in modifying the microstructure in the processed regions and, although the localized heating was applied to a single length of the wire, a non-uniform temperature distribution is obtained along that length, with implications in terms of graded functionality, as reported during in-situ experiments performed by Braz Fernandes *et al*. (2019). As a result of this graded microstructural

change along the heat treated segment, Sun *et al.* (2018) have used as a gauge length for tensile testing only the central 10 mm of the 90 mm long heat treated sample.

Recently, local processing methods have been used to control the microstructure and mechanical properties of shape memory alloys. Oliveira *et al.* (2016) used a laser heat source to control the grain size and texture in Cu-based shape memory alloys. Although effective, this method has the drawback of being expensive owing to the high investment required. Other authors were seen to use more economical methods to locally control the microstructure in shape memory alloys. Delville *et al.* (2010) used ultra-fast electrical pulse currents in cold-drawn NiTi parts. By varying the process parameters, which would influence the maximum temperature reached, and permanence time, the critical temperature where the material solid-state transformations can occur was varied. As a result, different microstructural features (grain size and existing phases) were obtained and as a consequence, the mechanical behaviour was altered.

The importance of evaluation techniques for characterization and indirect identification of the phases that are present and their structural changes in shape memory alloys have been reported by Nascimento *et al.* (2020), which has developed an embedded fiber sensor to monitor temperature and strain of thermoplastics reinforced by pre-functionalized NiTi.

The functional properties of NiTi shape memory alloys make possible their use in multiple advanced engineering applications. However, these applications rely on monolithic-like properties. The ability to create and control the functional properties along a NiTi part can further boost the potential applications of these alloys. One critical issue arises when trying to obtain functionally graded materials based on NiTi alloys: the need for expensive and complex thermo/mechanical treatment. In this work we show that a simple and cost-effective method can be used to control the structure and mechanical properties in NiTi shape memory alloys. The introduction of electrical current and the subsequent Joule effect were used to perform short time heat treatments within the 300 to 400 °C temperature range in different segments of a given strip. The effect of process parameters on the transformation characteristics was assessed by thermography, electrical conductivity measurements, synchrotron X-ray diffraction and mechanical testing. It was observed that these localized and fast (< 10 minutes) heat treatments are effective in drastically changing the functional and transformation properties of NiTi shape memory alloys, thus opening new routes for their thermomechanical processing.

2. Process developments

Conventional heat treatments for shape memory alloys typically require the use of furnaces as exemplified by Mahmud *et al.* (2008), where a given temperature is homogenously applied in the material. Therefore, the creation of functionally graded properties induced by thermal heat treatments is extremely difficult. Recently, Delobelle *et al.* (2016) and Oliveira *et al.* (2016) were able to create functionally graded materials based on shape memory alloys using other heat sources, namely a laser beam. Though the laser beam spot can be significantly small, hence allowing for very fine customization of the material microstructure, the equipment required is expensive which can hinder its use in industrial applications. This subject was recently reviewed by Shariat *et al.* (2017).

To overcome the need to obtain functionally graded parts via the use of heat treatments, another option was considered: the imposition of an electrical current in between two electrodes that can selectively heat the material up to a target temperature and locally process it. This process variant has the advantage of allowing to locally control the material microstructure and is also highly cost-effective, in opposition to the use of laser-based systems. One potential drawback of this solution occurs when the targeted temperatures for the localized treatments surpass the material oxidation temperature. While in a furnace it is possible to include a protective atmosphere, during the heat treatments induced by Joule effect it may be required the development of a suitable protection enclosure to guarantee an oxidation-free material. Since the temperatures used in this work (maximum of 400 °C) are below the oxidation temperature of NiTi, the creation of a dedicated enclosure was not considered, though this is currently under development.

The prototype developed to produce a non-linear heat treatment along the length of a strip (or wire) by Joule effect is depicted in Figure 1 a). In the region to be heat treated, two copper electrodes are used for current injection. The material temperature will increase as a result of the Joule effect, and after a short period of time (~ 60 seconds) the maximum temperature, which will depend on the imposed current, is reached (Figure 1 b)). The prototype used in this investigation allows to select the length between electrodes, which represents the segment to be processed, and its position along the strip (or wire). Thus, independent heat treatments throughout the strip (or wire) can be produced. Preliminary tests were performed to determine the effect of electrical current on the maximum temperature reached. These results were then used to perform selective heat treatments between 300

and 400 °C, frequently used heat treatment temperatures for NiTi alloys. This dedicated equipment also has the possibility to make stationary, as well as dynamic heat treatments.

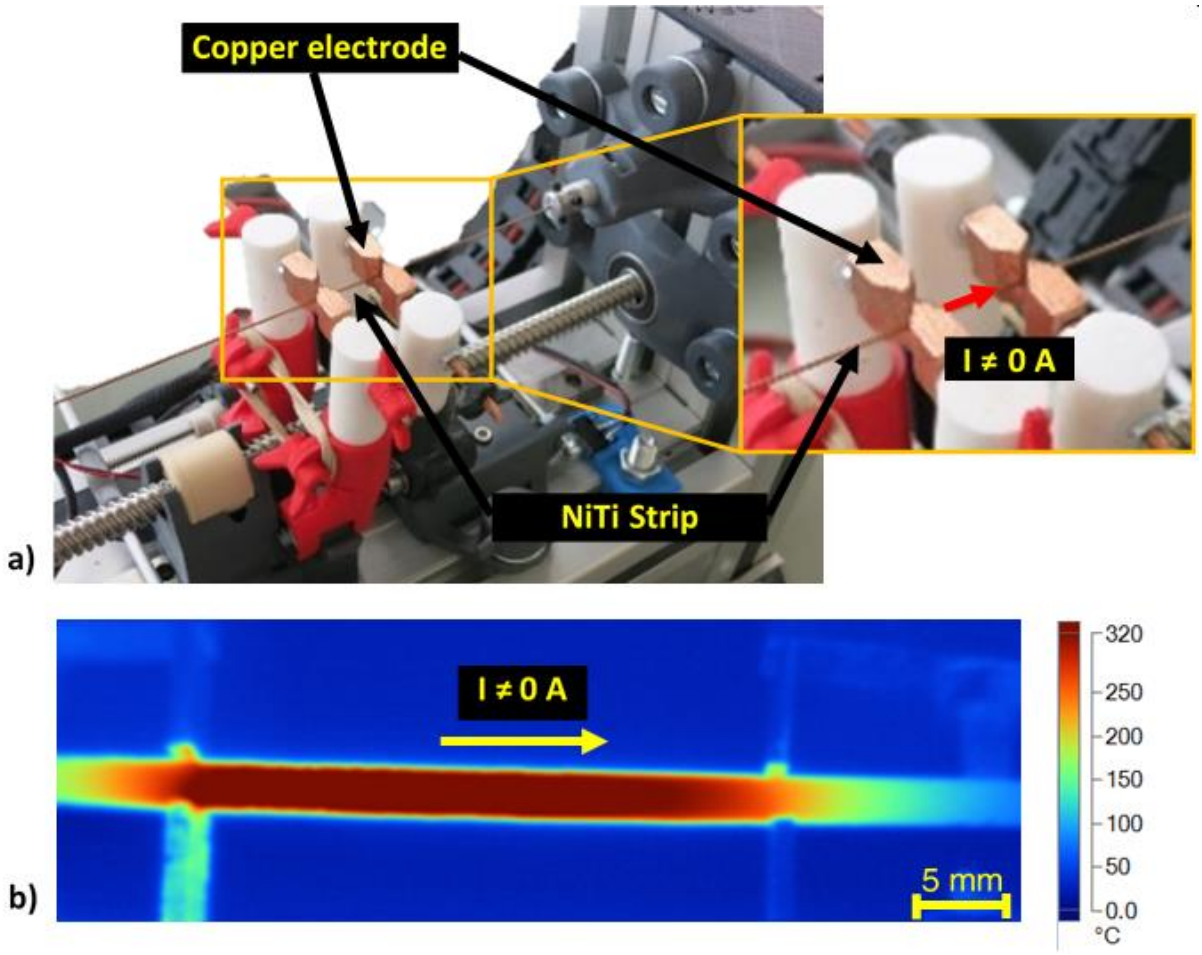

Figure 1 – Experimental apparatus:
a) Prototype for the production of FGM. b) Infrared image during heat treatment during a locally heat treatment corresponding to a segment of a FGM.

3. Materials and Methods

3.1. Production of functionally graded materials

In order to produce a functionally graded material (FGM), a cold-rolled NiTi strip (51 at% Ni) with a rectangular cross-section of 2.9 × 0.9 mm^2 was used. The total length of the strips was 256 mm. The as-received strips were selectively heat treated as schematically depicted in Figure 2 a): three regions of interest, each with a total length of 32 mm were heat treated by the application of different

electrical current intensities. The current was applied via two copper electrodes placed at the ends of the regions of interest to heat treat. During the creation of these FGMs, it was possible to control different processing parameters such as: length of the heat treated region; electrical current imposed to the material, which will determine the temperature experienced by the material; and the total time of the heat treatment. For each region of interest, the applied current was varied between 16.0 and 21.0 A, corresponding to 300 and 400 °C of maximum temperature, respectively, while the time was kept constant at 10 minutes. The distance between two consecutive regions of interest was 40 mm. The FGM is the result of the customization of the properties of each processed zone along the length of the strip.

The selected temperatures of 300, 350 and 400 ºC will promote the onset for recrystallization of the severely cold worked NiTi. However, due to the short time of these localized heat treatments, full recrystallization of the microstructure is never achieved. Typically, for such to occur, longer times (> 1 hour) or higher temperature (> 450 ºC) are required, as shown by Zhu *et al.* (2016).

To test the process reproducibility four different strips were heat treated and subsequentially characterized.

The temperature reached during each heat treatment was monitored using an infrared camera, Fluke Ti400. To minimize measurement errors due to changes in the material emissivity with temperature, the NiTi strips were coated with a black matt ink before the heat treatment, and a fixed value of 0.95 was used as the emissivity. Following this procedure, it was observed that the maximum temperature at the central point of the heat treated segment for 16.0, 18.6 and 21.0 A was 300, 350 and 400 °C, respectively. The heating and cooling behaviour of the material, as observed via infrared camera, is depicted in Figure 2 b). It must be noted that for each electrical current value, the corresponding maximum temperature was achieved in ~ 60 s after which the heat treatment enters a stationary state. It must also be observed that at the end of 10 minutes of heat treatment the temperature decay was not forced, that is, the material decreases its temperature by natural cooling in still air.

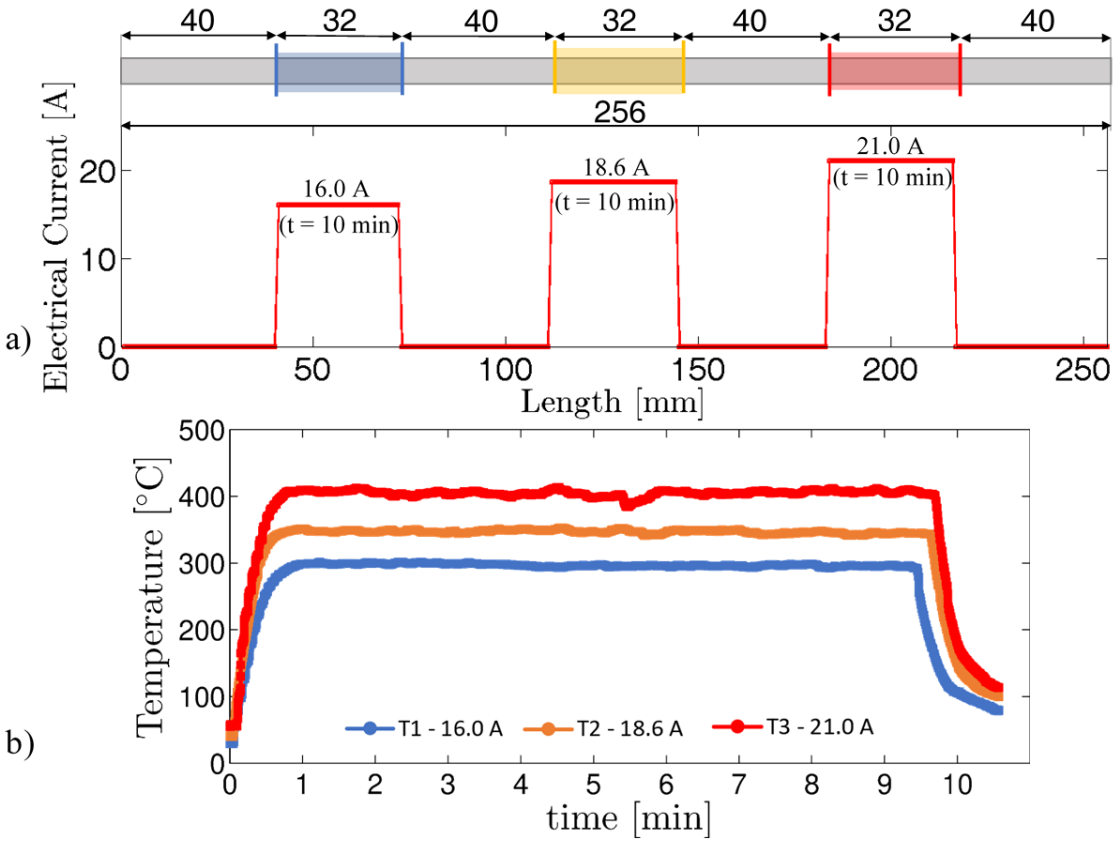

Figure 2 – Heat treatment plan for a FGM with 3 different customized regions: a) Parameters of the heat treatment. b) Temperature history in the midpoint of each heat treated segment obtained via infrared camera.

The temperature between electrodes was monitored during the heat treatments and the temperature profile for each heat treated segment during the stationary phase is depicted in Figure 3. The profile shows a parabolic trend with a maximum at the centre of the heat treated segment.

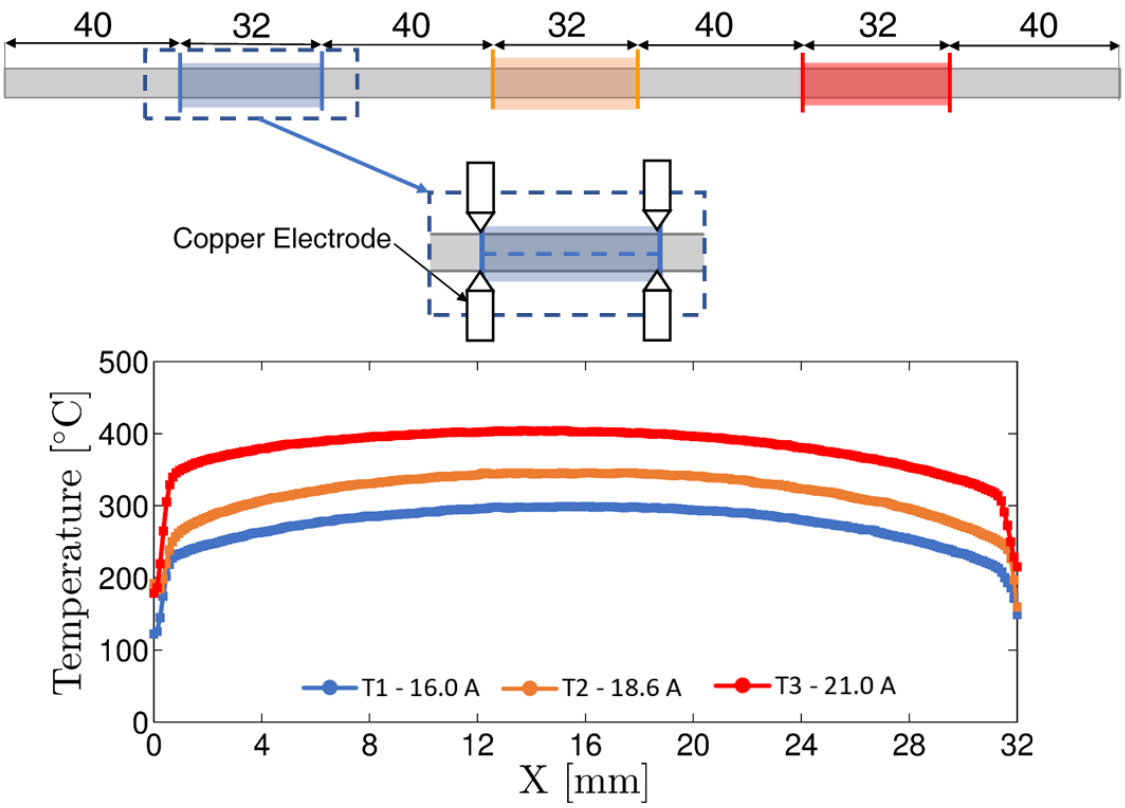

Figure 3 – Temperature profile of each heat treated segment after the stationary condition is reached.

3.2. Electrical Characterization

For shape memory alloys, a reliable and expedite way to characterize the existing phases is through the measurement of their electrical conductivity. Previously, T. G. Santos *et al.* (2011) used eddy currents for fine probing of the microstructure of thermomechanically processed metallic alloys. In this work, electrical characterization techniques were performed after the heat treatment to infer about potential phase changes in the processed regions caused by the selective heat treatments. These measurements were performed using contact or non-contact techniques as described below.

3.2.1. Eddy Currents testing

NiTi is an electrically conductive and non-ferromagnetic material that can be tested by eddy current technique. According to Rosado *et al.*, (2013, 2015), eddy current technique is sensitive to changes in electrical conductivity, magnetic permeability and lift-off (probe-to-sample distance). Since NiTi

is a non-ferromagnetic material and the probe used is not affected by lift-off, which is kept constant, the only property that changes is the electrical conductivity. Furthermore, the characterization can be performed without any contact between the probe and the specimen.

The customized probe developed and produced in this work to characterize the heat treated sections along the FGM is depicted in Figure 4 a. The eddy current generated by the customized probe in the strip is depicted in Figure 4 b). An impedance analyser NORTEC 500C was used for excitation and measurement of electrical impedance. A sweep along each strip was performed with a resolution of 100 µm and an excitation frequency of 1 MHz.

3.2.2. Four-point probe testing

Electrical resistivity, the inverse of electrical conductivity, can be measured using a dedicated probe or by 4-point probe method, as demonstrated in the work of Sorger *et al.* (2019). Both methods require contact with the sample and can be performed, in some cases, before, during and after the heat treatments.

A four-point probe was used to measure the electrical resistivity profile along the length of the strip. The probe has four straight aligned tungsten needles with a radius of 0.4 mm at the tip and they are equally distributed with 0.635 mm between them (Figure 4 c)). The excitation and measurements were performed using a Keithley SourceMeter 2450 that imposes a current intensity of 80 mA to the external needles, while simultaneously measuring the voltage in between the inner contacts with a sensitivity up to 10 nV (Figure 4 d)). The sweep along the complete processed material was performed with a resolution of 250 µm.

To evaluate the path of the electrical current for both techniques, numerical simulations were performed. The two setups were modelled and simulated in ANSYS Electronics software.

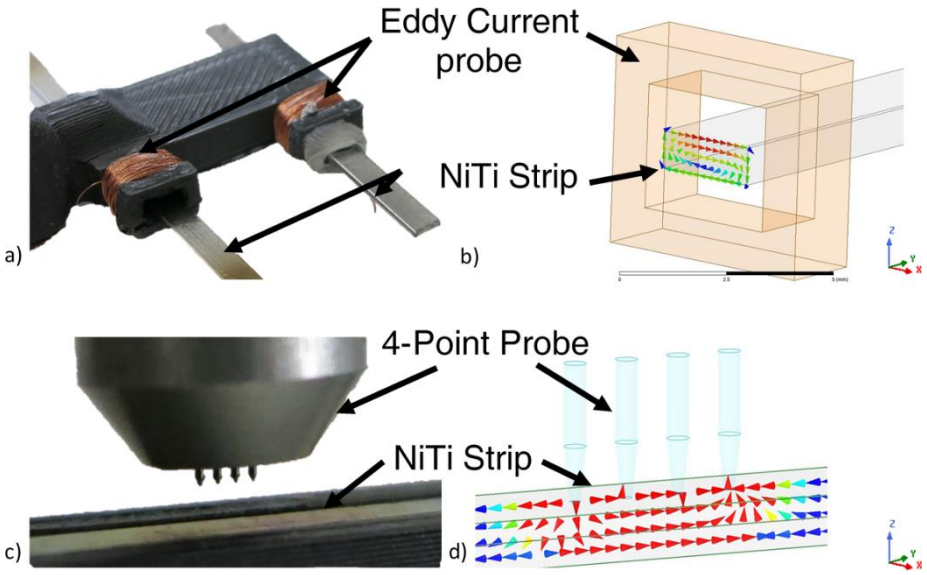

Figure 4 – Electrical characterization by eddy current and four-point probe testing. a) detail of differential eddy current customized probe. b) Numerical simulation of the eddy current field. c) detail of four-point probe. d) Numerical simulation of the current path using a four-point probe.

3.3. Characterization of electrical properties as a function of temperature

The produced FGM presents differences in its properties along the length that may be revealed in different ways. Changes in electrical conductivity can be indirectly evaluated using an infrared camera, as schematically depicted in Figure 5. The heat treatments may modify the electrical conductivity profile along the strip due to the formation of new phases and/or by changes of the material grain size and structural defects density as a result of recrystallization effects. The current injected into the material heats it by Joule effect; the existence of a gradient of electrical conductivity will impact the amount of heat generated along each processed region.

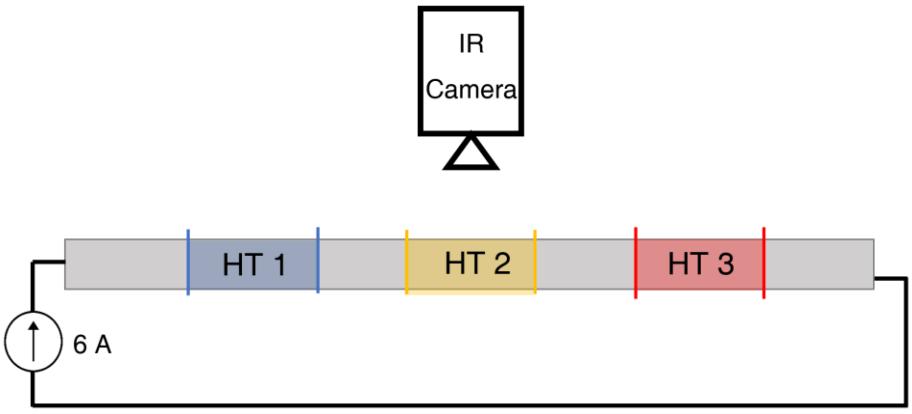

Figure 5 – Schematic of the measurement approach for identifying the different electrical conductivity zones along the length of the FGM, using an infrared camera and an imposed electrical current.

3.4. Uniaxial Tensile testing

To determine the mechanical properties of the functionally graded NiTi, uniaxial tensile testing was performed, in order to compare it with as-received strip. Typically, mechanical testing of shape memory alloys can be performed via conventional tensile testing to failure or by load/unload cycling.

An Autograph Shimadzu, model AG500Kng with a 50 kN load cell (SFLA-50Kn AG), was used to evaluate mechanical properties of the FGM and as-received strip. The gauge length was 60 mm for as-received strip and 256 mm for the produced FGM, and both trials were performed at 1 mm/min.

Additionally, a modified digital image correlation setup was used to measure the local strain over the FGM length. This encompassed marking the complete gauge length of the strips (which included the three processed regions) with lines duly spaced by 2 mm from one another, as schematically shown in Figure 6. Then, loading of the sample was performed up to 5% strain with increments of 1%. After each target strain was reached, a high-resolution photo was taken in order to selectively determine the local strain throughout each region of the material. This allows to determine which sections of the FGM are more deformed and correlate that mechanical behaviour with its structure.

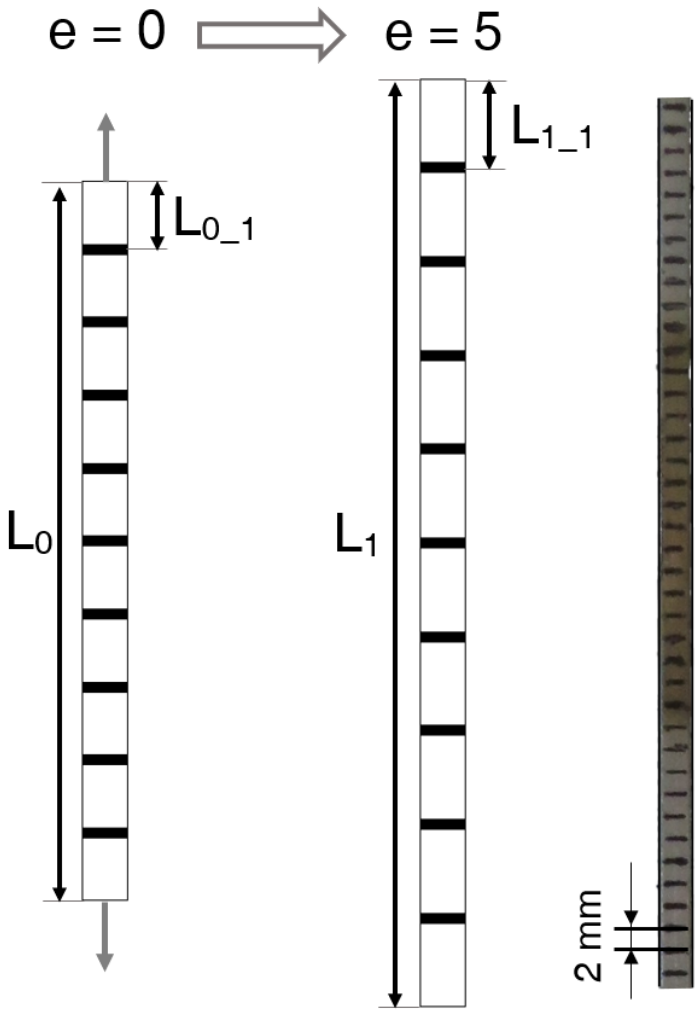

Figure 6 – Schematic for local strain measurements.

3.5. Differential scanning calorimetry

Differential scanning calorimetry (DSC), was used to determine the transformation temperatures of the material and infer about the existing phases in the material.

A *DSC 204 F1 Phoenix* model from *Netzsch* was used to perform a cycle at high and low temperature, using liquid nitrogen on low-temperature tests to cool down the system. The test was performed between - 150 °C and 150 °C with cooling and heating rate of 10 °C/min. Specimens (~10 mg) were obtained from the central part of each processed region and analysed. Prior to DSC, an etching solution of HF:HNO_3: H_20 (1:5:10 in volume) was used to remove the top surface layer which may be affected by the cutting process used to prepare the samples.

3.6. X-ray diffraction analysis

Synchrotron X-ray diffraction is a powerful characterization tool which allows, among other things, to determine the material crystal structure. With synchrotron radiation it is possible to obtain a high photon flux and significantly decrease the spot size allowing for characterization of the material structure with higher spatial resolution.

The synchrotron X-ray diffraction (XRD) measurements were performed at the High Energy Materials Science Beamline (HEMS) at PETRA III in DESY facilities (Hamburg, Germany). Radiation with a wavelength of 0.124 Å and energy of 98 keV was used. A Perkin-Elmer fast detector was used, and the sample-to-detector distance was kept at 1.4 m. A sweep along the strip was performed with 2 mm spacing. Treatment of the raw data was performed using freely available Fit2D software developed by Hammersley *et al.* (1996), following the procedure outlined in Oliveira *et al.* (2016).

4. Results and discussion

4.1. Electrical Characterization

During heat treatments, structural changes occur, and these can also be indirectly characterized by electrical properties measurement. After the FGM production, two complementary non-destructive techniques, four-point potential drop measurement, and eddy current technique were used.

4.1.1. Four-point probe testing

In this technique, the electrical conductivity is obtained by imposing an electrical current and measuring the voltage potential drop of the probe. Following equation 1 (Bowler, 2006), where t [m] is the material thickness, V [V] is the electrical voltage measured and I [A] the electrical current imposed, it is possible to determine the material electron conductivity, σ [S/m]. The sweep performed along the strip clearly depicts the presence of a FGM as shown in Figure 7.

$$\sigma = \frac{\ln 2}{\pi t}\left(\frac{\mathrm{I}}{\mathrm{V}}\right) \qquad \text{Equation 1}$$

The three heat treated segments were identified and their repeatability was demonstrated by testing two different strips and obtaining similar results. The non-processed segments have an electrical

conductivity of about 0.9 %IACS (International Annealed Copper Standard), while for the heat treated sections this value increases to nearly 1.05 %IACS. It may be beneficial for the functional behaviour of the material to present a graded transition between treated and non heat treated regions.

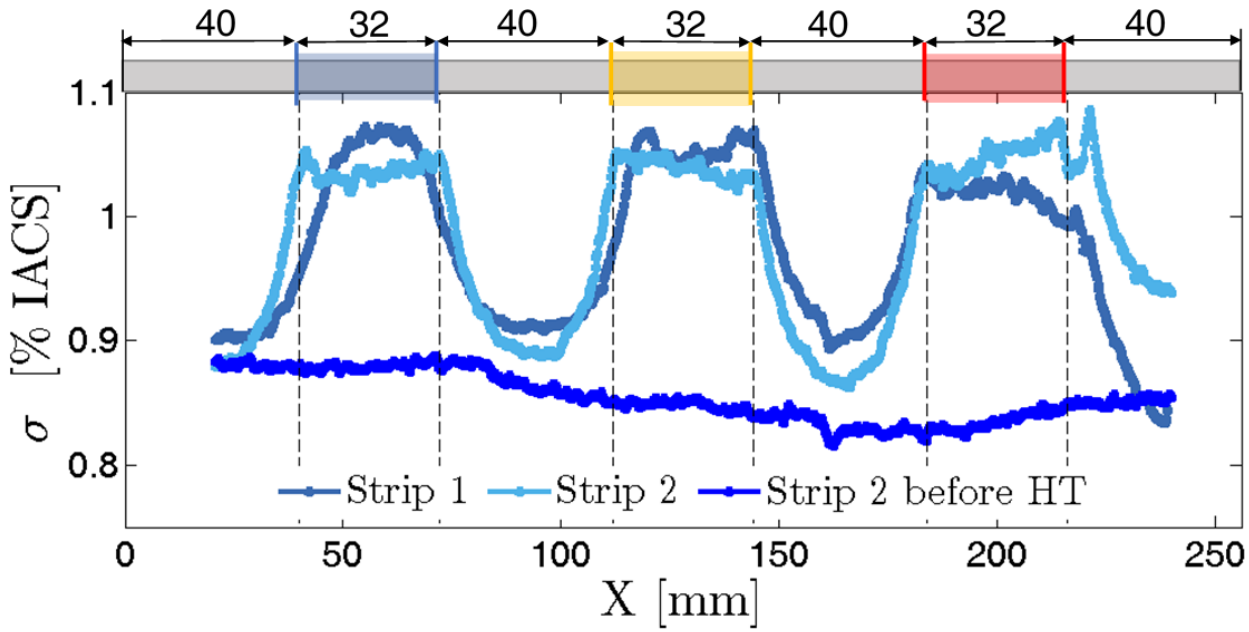

Figure 7 – Electrical conductivity profile of FGM using four-point probe testing at room temperature.

4.1.2. Eddy Currents testing

Unlike four-point probe measurements, eddy current testing is a technique without any contact between the probe and the tested material, and it measures differences in electrical conductivity, magnetic permeability and lift-off. The sweeps performed along the strips are shown in Figure 8 and demonstrate the suitability of the technique to evaluate the FGM produced, where a clear distinction between the different regions of the FGM was observed.

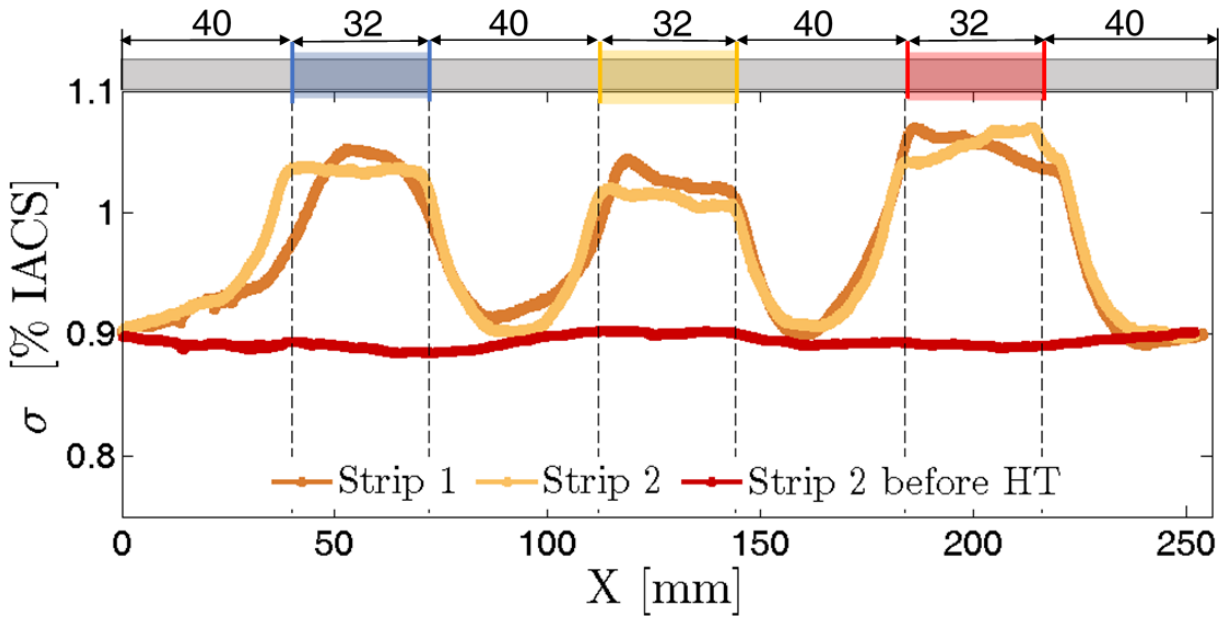

Figure 8 – Electrical conductivity profile of FGM using eddy current testing at room temperature.

Since NiTi is a non-magnetic alloy and the probe setup used is not affected by lift-off, the only difference measured by the probe is the electrical conductivity. Similarly, to the curves obtained for the four-point probe testing, a smooth transition between processed and non-processed segments is observed. Heterogeneities on the electrical conductivity profile inside the processed segments are also observed, and they are a consequence of the slight non-homogeneous temperature profile during the heat treatment.

The electrical conductivity in HT2 section is lower than in HT1 region suggesting that more than one phase is present in the processed segment at room temperature. To evaluate this possibility an electrical current of 6 A was imposed to rise the temperature of the strip to a level where only austenite can be present and a sweep was performed at this temperature (Figure 9). The electrical conductivity profile changed and clearly depicts a coherent gradient when comparing the different heat treated sections, that is, the electrical conductivity of HT3 is higher than HT2, which is higher than HT1.

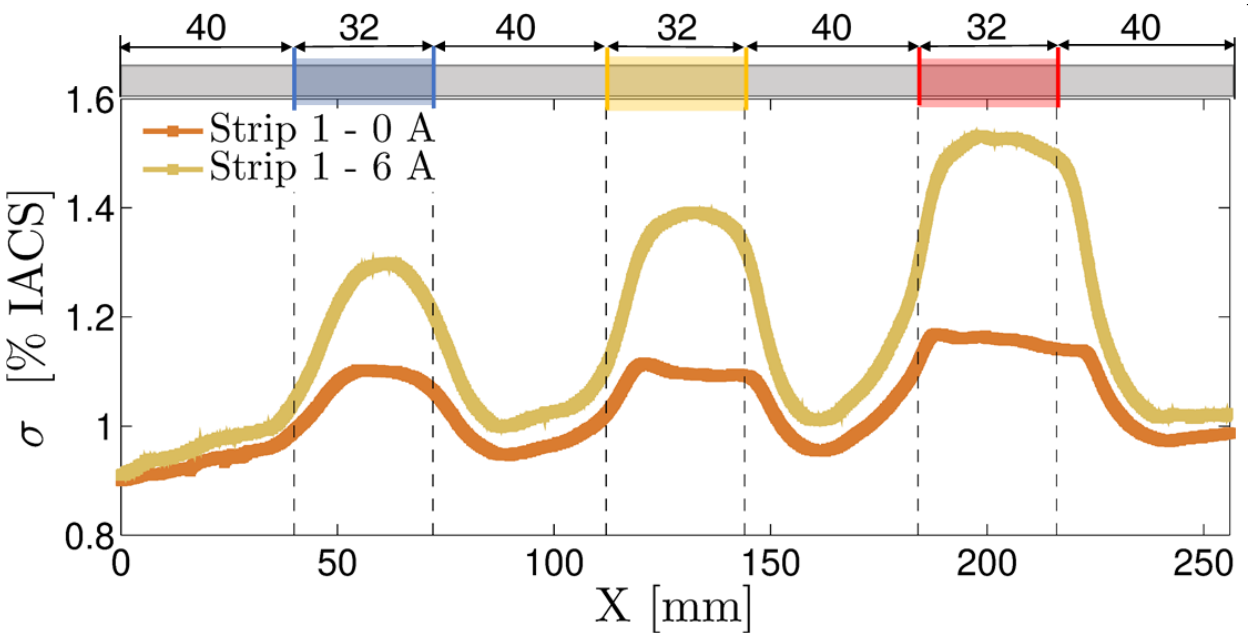

Figure 9 – Electrical conductivity profile of FGM using eddy current testing for room temperature (I = 0 A) and 90 °C (I = 6 A).

Since both four-point probe and eddy current testing were suitable to measure electrical conductivity, a comparison using both techniques was made, and this is shown in Figure 10. The two electrical profiles show good similarity and confirm that eddy current testing is an expedited and reliable technique for a fast determination of the electrical profile along the strip. As it will be seen later, it is then possible to correlate the material structure with the observed electrical profiles.

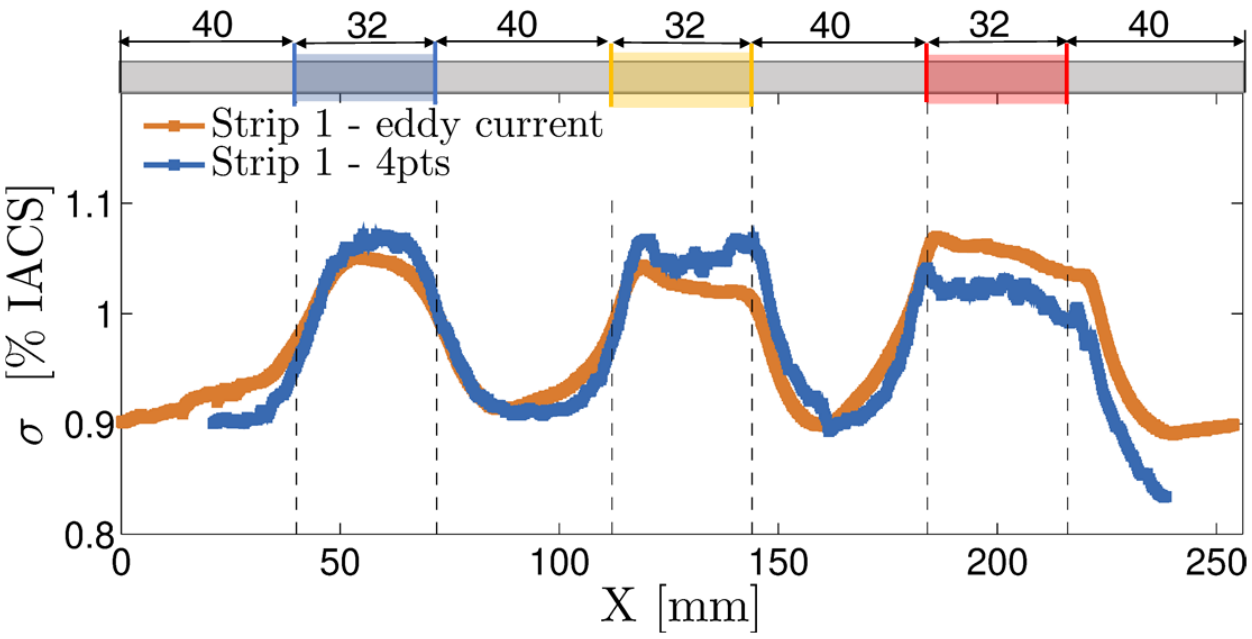

Figure 10 – Comparison of electrical conductivity profile of FGM using eddy current testing and four-point probe testing.

4.2. Thermal Characterization of electrical properties

Another method to evaluate electrical conductivity is through the visualization of the temperature profile, after FGM production, when a given current is applied to the material and its temperature raise by Joule effect. A current of 6 A was applied so that the temperature in the non-processed regions would reach approximately 90 °C. Regarding this characterization, a higher electrical conductivity corresponds to a decrease of the Joule effect heating, and consequently a lower temperature. The temperature profile is presented in Figure 11 and a clear distinction between processed and non-processed FGM regions is observed. Additionally, it can be observed that all processed regions have different maximum temperatures. In particular, the temperature in section HT1 is higher than in HT3, which implies that HT3 has higher electrical conductivity after the heat treatment and, in fact, this was observed, as reported in Figure 9. For shape memory alloys, heat treatments are mainly used to promote recrystallization and promote preferential precipitation which can drastically modify the transformation temperatures. These differences can be attributed to the structural-induced changes due to the heat treatment conditions selected. Overall, the FGM characteristics is clearly identified and each segment characterized via thermal analysis.

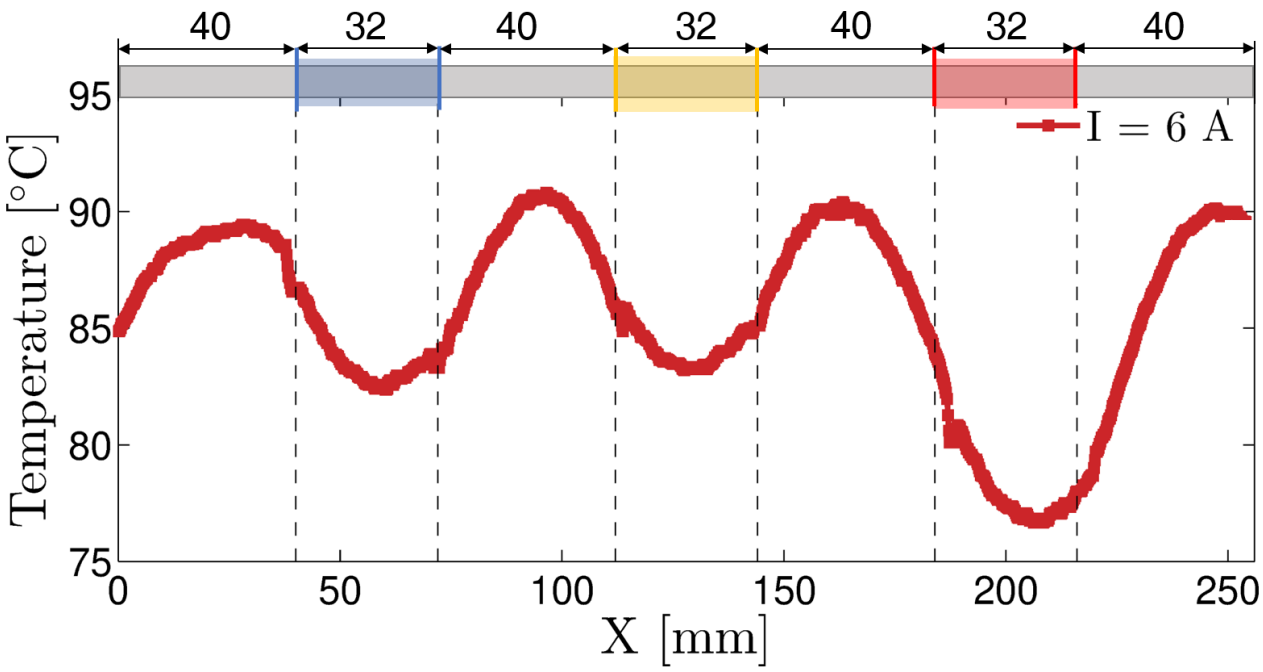

Figure 11 – Temperature profile of the FGM produced (Strip 1) using the methodology described in section 3.3. The electrical conductivity changes along the produced FGM and this implies different heat generation zones when an electrical current flow through the material.

4.3. Mechanical testing

The mechanical testing carried out in the FGM strip demonstrated a different behaviour when compared with as-received strip. As-received strip was in a cold worked condition, due to severe plastic deformation, as depicted in Figure 12. In fact, for this condition, no stress plateau was identified. On the other hand, in FGM stress-strain curve (Figure 13), a stress plateau was observed between approximately 1% to 2% of nominal strain.

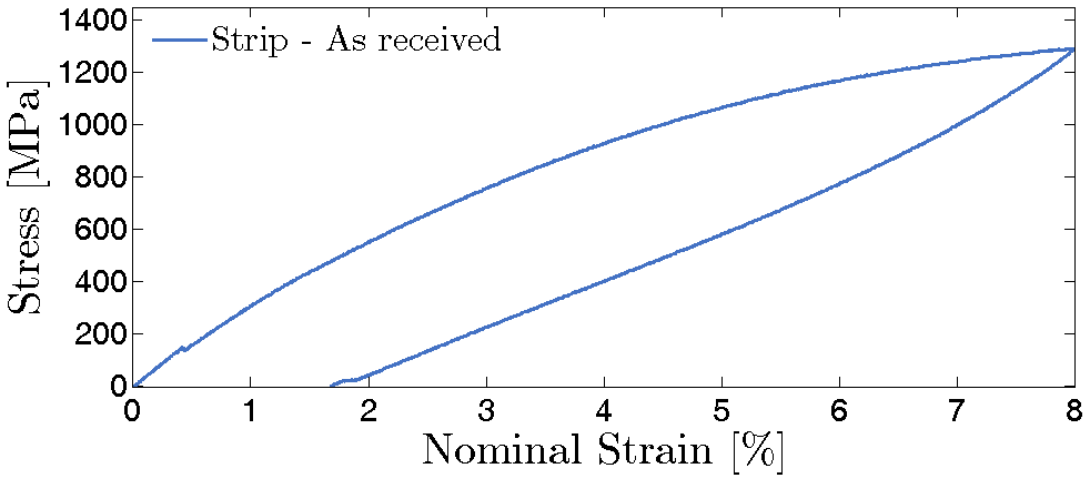

Figure 12 – Stress-strain curve of strip as received.

Mechanical testing by loading up to 5% strain and unloading to a zero-stress condition was performed using a modified digital image correlation procedure as described before. The stress-strain curve for this trial was depicted in Figure 13. While pulling the strip, two stops were made to take a high-resolution photo, first at nominal extension of 1 % and the second at nominal extension of 5 %. The distance between the lines drawn was measured before and during the testing were measured in order to evaluate the local strain at each point. The strain profile along the strip is depicted in Figure 14.

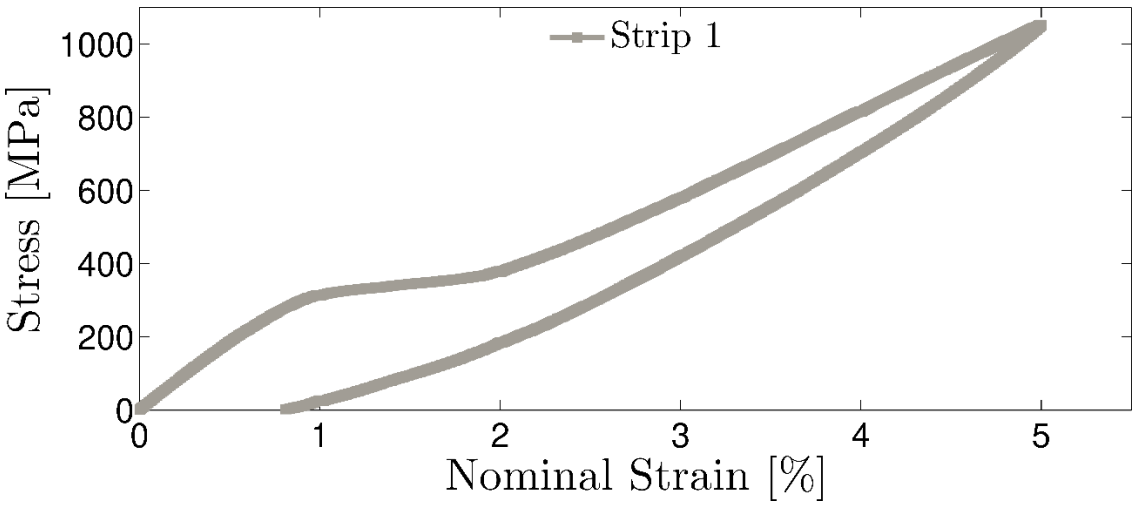

Figure 13 – Stress-strain curve of tensile test performed during the digital image correlation procedure.

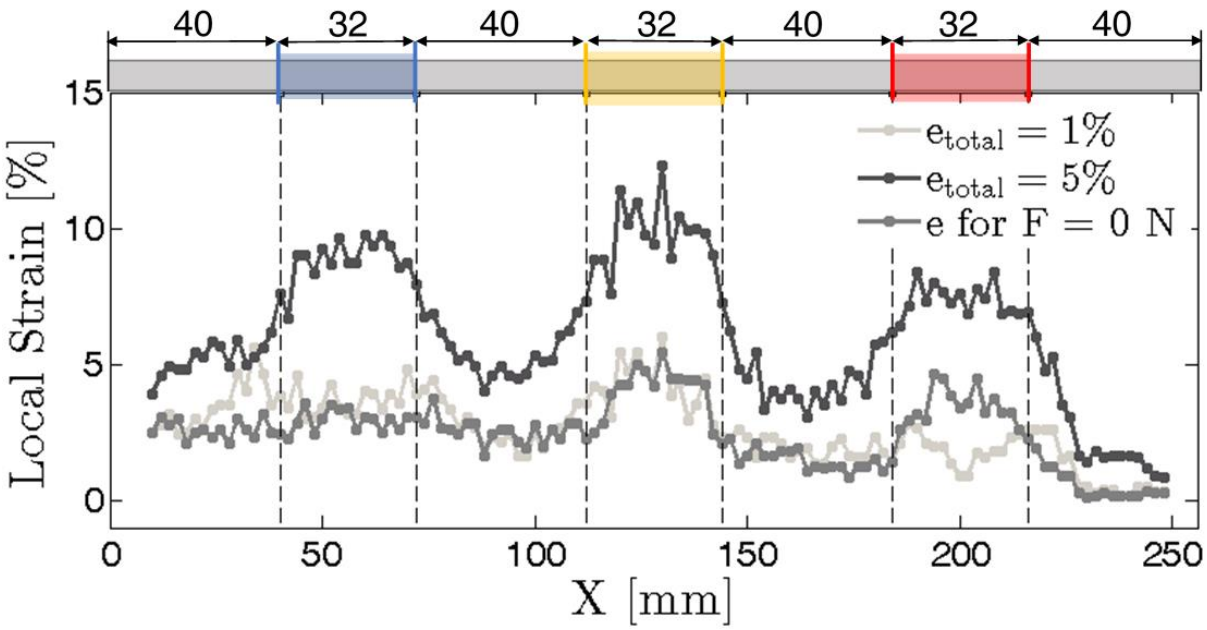

Figure 14 – Local strain profile of FGM using uniaxial tensile testing.

For a nominal extension of 1 %, only a slight increase of local strain was observed in HT2, however, when nominal extension reaches the maximum value of 5 %, it was found that local strain is higher in the processed zones. These zones have higher local strain when compared with non heat treated zone, since non heat treated zones remain in a cold worked state. The differences between each heat treated zone were related with evolution of tranformation temperature promoted by heat treatment. Thus, it was observed that local strain of HT2 is higher than HT1 and HT3 was the lower one and, indeed, the R_s transformation temperature (Table 1) presents the same trend. This result shows that there is the possibility to customize segments along the strip obtaining a functional gradient.

Upon unloading to a zero-stress condition (e for F = 0 N), non-complete strain recovery occurs suggesting the occurrence of martensite stabilization.

4.4. Differential scanning calorimetry

Differential scanning calorimetry of each heat treated segment and as-received strip was performed with the transformation behaviour depicted in Figure 15. The transformation temperatures for each heat treatment condition are summarized in Table 1.

In the as-received strip, no transformation was observed upon cooling/heating. However, in heat treated segments, it was observed that upon cooling evidence of a single transformation peak occurs.

A two-step transformation is evident during heating and cooling with an intermediate step giving R-phase. For the lower heat treatment temperature (300 ºC) the two-step transformation is not so clearly depicted, but it becomes more clearly distinguishable for 350 and 400 ºC. That can be attributed to the fact that at low temperatures the transformation kinetics are slower, thus the formation of Ni_4Ti_3, typically associated with the formation of R-phase in NiTi, is reduced. At 350 and 400 ºC, the precipitation kinetics increases, allowing for a more significant presence of Ni_4Ti_3, even though the heat treatment duration is small (10 minutes). As a consequence, the two-step transformation is more evident for these processing conditions.

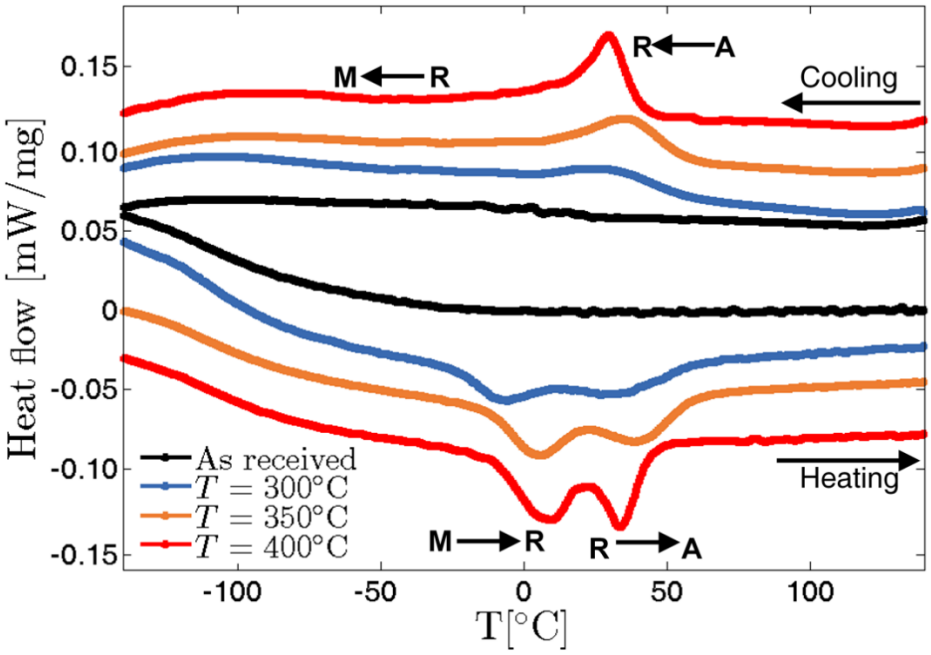

Figure 15 – Differential scanning calorimetry test.

At room temperature all processed regions have a mixture of both austenite, martensite and R-phase according to the DSC results. This explains why no complete recovery was obtained upon unloading the material to a zero-stress condition during the mechanical tests. Only, when the material is fully austenitic at the testing temperature, it is expected that complete strain recovery by superelasticity occurs. The stabilisation of martensite at the testing temperature prevents the full recovery of the FGM upon unloading, since during mechanical solicitation martensite is deformed and will keep

the imposed deformation, unless the material is heated above its austenite finishing temperature, triggering the shape memory effect.

Table 1 – Transition Temperature obtained by DSC.

		Transformation temperatures [ºC]					
		M_s	M_f	R_s	R_f	A_s	A_f
HT1 (300 °C)	Upon Cooling	- 50.8	< -150*	54.9	6.4	-	-
	Upon Heating	-	-	- 24.5	n.d.	16.5	56.9
HT2 (350 °C)	Upon Cooling	- 41.8	<- 150*	57.7	12.4	-	-
	Upon Heating	-	-	- 11.7	n.d.	18.3	58.8
HT3 (400 °C)	Upon Cooling	- 51.4	< -150*	41.5	15.3	-	-
	Upon Heating	-	-	- 10.2	n.d.	17.5	44.3

*Note: M_f is not characterized within the equipment temperature range.

4.5. X-ray diffraction testing

Synchrotron X-ray diffraction analysis was used for structural characterization of the processed NiTi strips. Figure 16 depicts the evolution of the 110 B2 austenite peak along the processed region. It can be observed that the intensity of the 110 B2 peak increases as the heat treatment temperature increases. An increase of peak maximum intensity accompanied by a decrease of the Full-Width at Half Maximum (FWHM) is related to the recrystallization effect induced by the localized heat treatment imposed to the cold-worked material.

The diffraction data is in good agreement with the DSC results, since the transformation peaks upon cooling shift to lower temperatures as the heat treatment temperature increases, which results in more austenite being stable at room temperature.

It can be observed that the non-processed material is composed of both martensite and austenite (Figure 16). A slight increase of the peak intensity of the R-phase is evident as the heat treatment temperature increases. This fraction of R-phase affects the electrical conductivity, since the electrical conductivity of the R-phase is lower than that of austenite. This effect, added to the recrystallization phenomenon induced by the heat treatments, can justify the fact that the same electrical conductivity level for HT2 and HT3 occurs at room temperature, as evidenced in Figure 7 and Figure 8.

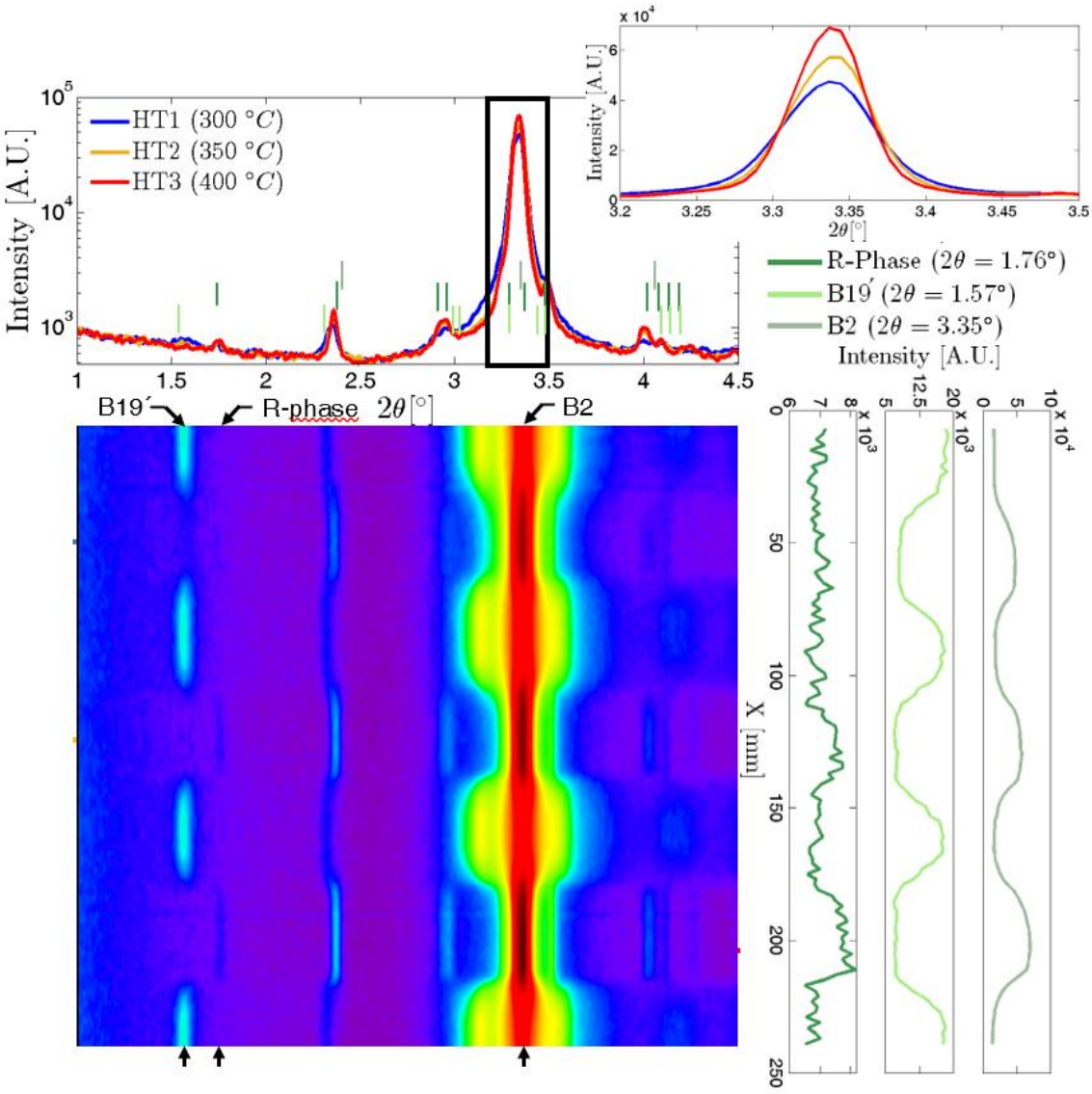

Figure 16 - Diffractogram and 2D plot profile of FGM using synchrotron X-ray diffraction.

5. Reading-key based on multiphenomena characterization

The structural characterization by means of different techniques performed on the NiTi strips to create a functional gradient of properties by localized heat treatments allows to build a reading key as depicted in Figure 17.

The structural changes made during the production of the FGM are clearly observed when multiple destructive and non-destructive testing are employed. Additionally, it is possible to build a reading key based on the different physical phenomena (thermal, electrical and structural) as depicted in

Figure 17. For example, when comparing the temperature variation due to Joule heating effect and the electrical conductivity profiles, it is easy to conclude that the processed zones have higher conductivity than the non-processed regions, thus resulting in a higher temperature increase for the non heat treated regions (lower electrical conductivity). Furthermore, the HT3 profile for the temperature increase by Joule heating effect suggests a higher recrystallization effect in the processed region, which is in good agreement with (i) the DSC analysis, where a narrower and higher A → R peak is observed (top curve of Figure 15), as well as (ii) the synchrotron X-ray diffraction analysis, where a higher peak intensity for the (110) austenite is observed (Figure 16).

The two techniques that can measure electrical conductivity, four-point probe and eddy current testing, present the same profile, proving that both are reliable and expedite techniques. The main differences between four-point probe testing and eddy current technique is that in the former one a DC current was used and the probe is in contact with the material, while for the latter one an AC current is used, and no contact with the material under inspection exists.

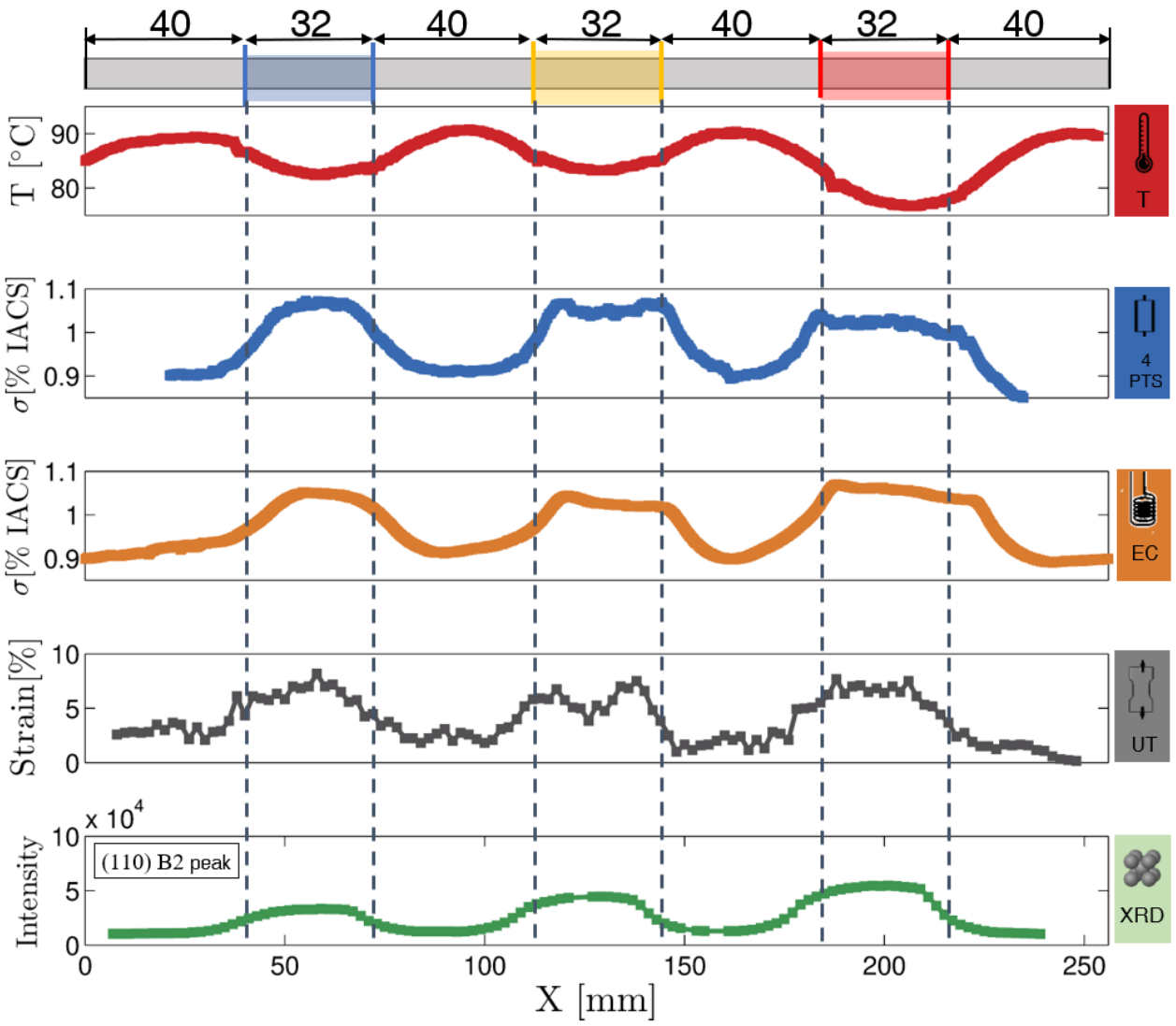

Figure 17 – Overview of all techniques used for FGM characterization. From top to bottom: temperature variation by Joule heating effect, electrical conductivity by 4-point probe, electrical conductivity by eddy-current, local strains at maximum global strain (5 %) and intensity profile of B2 (110) peak by XRD analysis.

6. Conclusions

In this work, functionally graded parts were created by promoting localized short heat treatment schedules, by Joule effect, to selectively tune the material structure and control transformation temperatures in NiTi shape memory alloys. The main conclusions of this work were:

(1) A set of NDE procedures was applied to assess the electrical characteristics of a functionally graded NiTi strip.

(2) The analysis of the electrical characteristics by techniques based on different physical principles (eddy-currents and 4-probe method) has given consistent results for the structural variations resulting from different localized treatments.

(3) The thermographic analysis has put in evidence the differentiated Joule heating effect at non-heat treated and heat treated segments, revealing its capability to identify structural variations related to the functional gradients of the strips. The results are also consistent with the electrical characterization by eddy-currents and 4-probe method.

(4) The unusual heat treatment setup can be used to control the structure and transformation temperatures in NiTi shape memory alloys, avoiding the need for highly expensive processing techniques, such as those based on lasers, and an in-line qualitative analysis of the existing phases on NiTi can be achieved by inexpensive and expedite eddy current testing.

Acknowledgments

The authors gratefully acknowledge the funding of Project POCI-01-0145-FEDER-016414 (FIBR3D), cofinanced by Programa Operacional Competitividade e Internacionalização and Programa Operacional Regional de Lisboa, through Fundo Europeu de Desenvolvimento Regional (FEDER) and by National Funds through FCT - Fundação para a Ciência e a Tecnologia. PLI, JPO and TGS acknowledge Fundação para a Ciência e a Tecnologia (FCT - MCTES) for its financial support via the project UID/00667/2020 (UNIDEMI). PLI would like to acknowledge Fundação para a Ciência e a Tecnologia for its financial support via the PhD scholarship FCT-SFRH/BD/146885/2019. FMBF acknowledges funding of CENIMAT by FEDER through the program COMPETE 2020 and National Funds through FCT-Portuguese Foundation for Science and Technology, under the project UID/CTM/50025/2019 and FCT/MCTES. Parts of this research

were carried out at beamline P-07-HEMS at DESY, a member of the Helmholtz Association. The research leading to this result has been supported by the Project CALIPSOplus under the Grant Agreement 730872 from the EU Framework Programme for Research and Innovation HORIZON 2020.

References

Bowler, N., 2006. Theory of four-point direct-current potential drop measurements on a metal plate. Res. Nondestruct. Eval. 17, 29–48. https://doi.org/10.1080/09349840600582092

Braz Fernandes, F.M., Camacho, E., Rodrigues, P.F., Inácio, P., Santos, T.G., Schell, N., 2019. In Situ Structural Characterization of Functionally Graded Ni–Ti Shape Memory Alloy During Tensile Loading. Shape Mem. Superelasticity 5, 457–467. https://doi.org/10.1007/s40830-019-00237-2

Delobelle, V., Chagnon, G., Favier, D., Alonso, T., 2016. Study of electropulse heat treatment of cold worked NiTi wire: From uniform to localised tensile behaviour. J. Mater. Process. Technol. 227, 244–250. https://doi.org/10.1016/J.JMATPROTEC.2015.08.011

Delville, R., Malard, B., Pilch, J., Sittner, P., Schryvers, D., 2010. Microstructure changes during non-conventional heat treatment of thin Ni–Ti wires by pulsed electric current studied by transmission electron microscopy. Acta Mater. 58, 4503–4515. https://doi.org/10.1016/J.ACTAMAT.2010.04.046

Hammersley, A.P., Svensson, S.O., Hanfland, M., Fitch, A.N., Häusermann, D., 1996. Two-dimensional detector software: From real detector to idealised image or two-theta scan. High Press. Res. 14, 235–248. https://doi.org/10.1080/08957959608201408

Kang, S.W., Cho, G.B., Yang, S.Y., Liu, Y., Yang, H., Miyazaki, S., Nam, T.H., 2010. Transformation temperatures and shape memory characteristics of a Ti-45Ni-5Cu(at%) alloy annealed by Joule heating. Phys. Scr. T T139. https://doi.org/10.1088/0031-8949/2010/T139/014068

Mahmud, A.S., Liu, Y., Nam, T.H., 2008. Gradient anneal of functionally graded NiTi. Smart Mater. Struct. 17. https://doi.org/10.1088/0964-1726/17/01/015031

Meng, Q., Wu, Z., Bakhtiari, R., Zhang, J., Yang, H., Liu, Y., 2016. Stress serration and arch-shaped Lüders stress plateau behaviour of Ti-50.8 at% Ni wire prepared by selective electrical resistance over-aging. Smart Mater. Struct. 25. https://doi.org/10.1088/0964-1726/25/11/115035

Meng, Q., Yang, H., Liu, Y., Nam, T., Favier, D., 2013. Ti–50.8 at.% Ni wire with variable mechanical properties created by spatial electrical resistance over-ageing. J. Alloys Compd. 577, S245–S250. https://doi.org/10.1016/J.JALLCOM.2012.02.131

Nascimento, M., Inácio, P., Paixão, T., Camacho, E., Novais, S., Santos, T.G., Fernandes, F.M.B., Pinto, J.L., 2020. Embedded fiber sensors to monitor temperature and strain of polymeric parts fabricated by additive manufacturing and reinforced with NiTi wires. Sensors (Switzerland) 20. https://doi.org/10.3390/s20041122

Oliveira, J.P., Braz Fernandes, F.M., Miranda, R.M., Schell, N., Ocaña, J.L., 2016a. Effect of laser welding parameters on the austenite and martensite phase fractions of NiTi. Mater. Charact. 119, 148–151. https://doi.org/10.1016/J.MATCHAR.2016.08.001

Oliveira, J.P., Zeng, Z., Omori, T., Zhou, N., Miranda, R.M., Fernandes, F.M.B., 2016b. Improvement of damping properties in laser processed superelastic Cu-Al-Mn shape memory alloys. Mater. Des. 98, 280–284. https://doi.org/10.1016/J.MATDES.2016.03.032

Rosado, L.S., Gonzalez, J.C., Santos, T.G., Ramos, P.M., Piedade, M., 2013. Geometric optimization of a differential planar eddy currents probe for non-destructive testing. Sensors Actuators A Phys. 197, 96–105. https://doi.org/10.1016/J.SNA.2013.04.010

Rosado, L.S., Santos, T.G., Ramos, P.M., Vilaça, P., Piedade, M., 2015. A new dual driver planar eddy current probe with dynamically controlled induction pattern. NDT E Int. 70, 29–37. https://doi.org/10.1016/J.NDTEINT.2014.09.009

Santos, Telmo G., Miranda, R.M., Vilaça, P., Teixeira, J.P., 2011. Modification of electrical conductivity by friction stir processing of aluminum alloys. Int. J. Adv. Manuf. Technol. 57, 511–519. https://doi.org/10.1007/s00170-011-3308-4

Santos, T. G., Miranda, R.M., Vilaça, P., Teixeira, J.P., dos Santos, J., 2011. Microstructural mapping of friction stir welded AA 7075-T6 and AlMgSc alloys using electrical conductivity. Sci. Technol. Weld. Join. 16, 630–635. https://doi.org/10.1179/1362171811Y.0000000052

Shariat, B.S., Meng, Q., Mahmud, A.S., Wu, Z., Bakhtiari, R., Zhang, J., Motazedian, F., Yang, H., Rio, G., Nam, T., Liu, Y., 2017. Functionally graded shape memory alloys: Design, fabrication and experimental evaluation. Mater. Des. 124, 225–237. https://doi.org/10.1016/J.MATDES.2017.03.069

Sorger, G.L., Oliveira, J.P., Inácio, P.L., Enzinger, N., Vilaça, P., Miranda, R.M., Santos, T.G., 2019. Non-destructive microstructural analysis by electrical conductivity: Comparison with hardness measurements in different materials. J. Mater. Sci. Technol. 35, 360–368. https://doi.org/10.1016/J.JMST.2018.09.047

Sun, B., Lin, J., Fu, M.W., 2018. Dependence of processing window and microstructural evolution on initial material state in direct electric resistance heat treatment of NiTi alloy. Mater. Des. 139, 549–564. https://doi.org/10.1016/J.MATDES.2017.11.044

Wang, Y.B., Zheng, Y.F., Liu, Y., 2009. Effect of short-time direct current heating on phase transformation and superelasticity of Ti-50.8at.%Ni alloy. J. Alloys Compd. 477, 764–767. https://doi.org/10.1016/j.jallcom.2008.10.131

Yang, S. yong, Kang, S. won, Lim, Y.M., Lee, Y. jung, Kim, J. il, Nam, T. hyun, 2010. Temperature profiles in a Ti-45Ni-5Cu (at%) shape memory alloy developed by the Joule heating. J. Alloys Compd. 490. https://doi.org/10.1016/j.jallcom.2009.10.069

Zhu, R., Jiang, Y., Guan, L., Li, H., Tang, G., 2016. Difference in recrystallization between electropulsing-treated and furnace-treated NiTi alloy. J. Alloys Compd. 658, 548–554. https://doi.org/10.1016/j.jallcom.2015.10.239